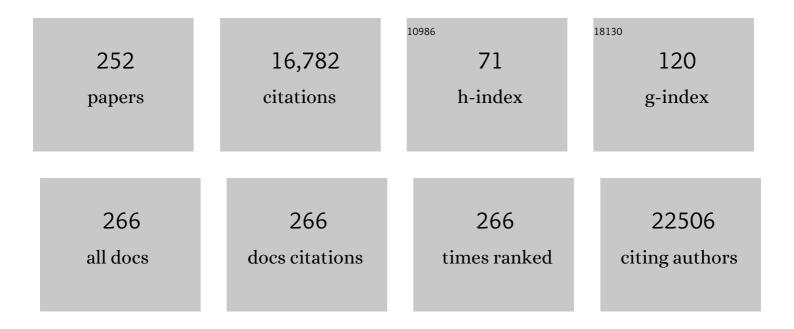
Gabriel M Veith

List of Publications by Year in descending order

Source: https://exaly.com/author-pdf/4878552/publications.pdf Version: 2024-02-01



#	Article	IF	CITATIONS
1	Water desalination using nanoporous single-layer graphene. Nature Nanotechnology, 2015, 10, 459-464.	31.5	1,372
2	Mixed Close-Packed Cobalt Molybdenum Nitrides as Non-noble Metal Electrocatalysts for the Hydrogen Evolution Reaction. Journal of the American Chemical Society, 2013, 135, 19186-19192.	13.7	897
3	CO Oxidation on Supported Single Pt Atoms: Experimental and ab Initio Density Functional Studies of CO Interaction with Pt Atom on 1,-Al ₂ O ₃ (010) Surface. Journal of the American Chemical Society, 2013, 135, 12634-12645.	13.7	535
4	Lithium salts for advanced lithium batteries: Li–metal, Li–O ₂ , and Li–S. Energy and Environmental Science, 2015, 8, 1905-1922.	30.8	460
5	A Superacid-Catalyzed Synthesis of Porous Membranes Based on Triazine Frameworks for CO ₂ Separation. Journal of the American Chemical Society, 2012, 134, 10478-10484.	13.7	408
6	Direct exfoliation of natural graphite into micrometre size few layers graphene sheets using ionic liquids. Chemical Communications, 2010, 46, 4487.	4.1	295
7	Controlled Synthesis of Mesoporous Carbon Nanostructures via a "Silica-Assisted―Strategy. Nano Letters, 2013, 13, 207-212.	9.1	248
8	Intrinsic thermodynamic and kinetic properties of Sb electrodes for Li-ion and Na-ion batteries: experiment and theory. Journal of Materials Chemistry A, 2013, 1, 7985.	10.3	226
9	Selective Oxidation of Glycerol under Acidic Conditions Using Gold Catalysts. Angewandte Chemie - International Edition, 2010, 49, 4499-4502.	13.8	222
10	Rational Design of Bi Nanoparticles for Efficient Electrochemical CO ₂ Reduction: The Elucidation of Size and Surface Condition Effects. ACS Catalysis, 2016, 6, 6255-6264.	11.2	212
11	Electrochemical and rate performance study of high-voltage lithium-rich composition: Li1.2Mn0.525Ni0.175Co0.1O2. Journal of Power Sources, 2012, 199, 220-226.	7.8	210
12	Germanium as negative electrode material for sodium-ion batteries. Electrochemistry Communications, 2013, 34, 41-44.	4.7	206
13	Pdâ€modified Au on Carbon as an Effective and Durable Catalyst for the Direct Oxidation of HMF to 2,5â€Furandicarboxylic Acid. ChemSusChem, 2013, 6, 609-612.	6.8	202
14	<i>In Situ</i> Doping Strategy for the Preparation of Conjugated Triazine Frameworks Displaying Efficient CO ₂ Capture Performance. Journal of the American Chemical Society, 2016, 138, 11497-11500.	13.7	200
15	Taming interfacial electronic properties of platinum nanoparticles on vacancy-abundant boron nitride nanosheets for enhanced catalysis. Nature Communications, 2017, 8, 15291.	12.8	200
16	High performance electrodes in vanadium redox flow batteries through oxygen-enriched thermal activation. Journal of Power Sources, 2015, 294, 333-338.	7.8	189
17	Characterization of sodium ion electrochemical reaction with tin anodes: Experiment and theory. Journal of Power Sources, 2013, 234, 48-59.	7.8	186
18	In Situ Ambient Pressure X-ray Photoelectron Spectroscopy Studies of Lithium-Oxygen Redox Reactions. Scientific Reports, 2012, 2, 715.	3.3	180

#	Article	IF	CITATIONS
19	Thermal stability and catalytic activity of gold nanoparticles supported on silica. Journal of Catalysis, 2009, 262, 92-101.	6.2	170
20	Determination of the Solid Electrolyte Interphase Structure Grown on a Silicon Electrode Using a Fluoroethylene Carbonate Additive. Scientific Reports, 2017, 7, 6326.	3.3	157
21	Lab-in-a-Shell: Encapsulating Metal Clusters for Size Sieving Catalysis. Journal of the American Chemical Society, 2014, 136, 11260-11263.	13.7	152
22	Elucidating the Phase Transformation of Li ₄ Ti ₅ O ₁₂ Lithiation at the Nanoscale. ACS Nano, 2016, 10, 4312-4321.	14.6	144
23	Electrochemical and Solid-State Lithiation of Graphitic C ₃ N ₄ . Chemistry of Materials, 2013, 25, 503-508.	6.7	141
24	Surface chemistry of metal oxide coated lithium manganese nickel oxide thin film cathodes studied by XPS. Electrochimica Acta, 2013, 90, 135-147.	5.2	140
25	Characterisation of gold catalysts. Chemical Society Reviews, 2016, 45, 4953-4994.	38.1	140
26	Cobalt Molybdenum Oxynitrides: Synthesis, Structural Characterization, and Catalytic Activity for the Oxygen Reduction Reaction. Angewandte Chemie - International Edition, 2013, 52, 10753-10757.	13.8	139
27	Calendar aging of silicon-containing batteries. Nature Energy, 2021, 6, 866-872.	39.5	137
28	Sonochemical functionalization of mesoporous carbon for uranium extraction from seawater. Journal of Materials Chemistry A, 2013, 1, 3016.	10.3	132
29	Nanoporous Ionic Organic Networks: Stabilizing and Supporting Gold Nanoparticles for Catalysis. Nano Letters, 2015, 15, 823-828.	9.1	132
30	Surface studies of high voltage lithium rich composition: Li1.2Mn0.525Ni0.175Co0.1O2. Journal of Power Sources, 2012, 216, 179-186.	7.8	131
31	Gold Nanoparticles Supported on Carbon Nitride: Influence of Surface Hydroxyls on Low Temperature Carbon Monoxide Oxidation. ACS Catalysis, 2012, 2, 1138-1146.	11.2	127
32	Direct Determination of Solid-Electrolyte Interphase Thickness and Composition as a Function of State of Charge on a Silicon Anode. Journal of Physical Chemistry C, 2015, 119, 20339-20349.	3.1	127
33	Influence of Lithium Salts on the Discharge Chemistry of Li–Air Cells. Journal of Physical Chemistry Letters, 2012, 3, 1242-1247.	4.6	123
34	Mo3Sb7 as a very fast anode material for lithium-ion and sodium-ion batteries. Journal of Materials Chemistry A, 2013, 1, 11163.	10.3	121
35	Cu2Sb thin films as anode for Na-ion batteries. Electrochemistry Communications, 2013, 27, 168-171.	4.7	115
36	Superior Conductive Solid-like Electrolytes: Nanoconfining Liquids within the Hollow Structures. Nano Letters, 2015, 15, 3398-3402.	9.1	115

#	Article	IF	CITATIONS
37	Spectroscopic Characterization of Solid Discharge Products in Li–Air Cells with Aprotic Carbonate Electrolytes. Journal of Physical Chemistry C, 2011, 115, 14325-14333.	3.1	114
38	Hydrogen evolution at the negative electrode of the all-vanadium redox flow batteries. Journal of Power Sources, 2014, 248, 560-564.	7.8	113
39	Understanding the Low-Voltage Hysteresis of Anionic Redox in Na ₂ Mn ₃ O ₇ . Chemistry of Materials, 2019, 31, 3756-3765.	6.7	112
40	Polymerized Ionic Networks with High Charge Density: Quasiâ€Solid Electrolytes in Lithiumâ€Metal Batteries. Advanced Materials, 2015, 27, 8088-8094.	21.0	110
41	Sol immobilization technique: a delicate balance between activity, selectivity and stability of gold catalysts. Catalysis Science and Technology, 2013, 3, 3036.	4.1	109
42	The reaction mechanism of SnSb and Sb thin film anodes for Na-ion batteries studied by X-ray diffraction, 119Sn and 121Sb Mössbauer spectroscopies. Journal of Power Sources, 2014, 267, 329-336.	7.8	109
43	Probing the electrode/electrolyte interface in the lithium excess layered oxide Li1.2Ni0.2Mn0.6O2. Physical Chemistry Chemical Physics, 2013, 15, 11128.	2.8	107
44	Silica-Supported Au–CuO _{<i>x</i>} Hybrid Nanocrystals as Active and Selective Catalysts for the Formation of Acetaldehyde from the Oxidation of Ethanol. ACS Catalysis, 2012, 2, 2537-2546.	11.2	105
45	Highly dispersed sulfur in a porous aromatic framework as a cathode for lithium–sulfur batteries. Chemical Communications, 2013, 49, 4905.	4.1	103
46	A Novel Electrolyte Salt Additive for Lithiumâ€lon Batteries with Voltages Greater than 4.7 V. Advanced Energy Materials, 2017, 7, 1601397.	19.5	103
47	Low-Temperature Fluorination of Soft-Templated Mesoporous Carbons for a High-Power Lithium/Carbon Fluoride Battery. Chemistry of Materials, 2011, 23, 4420-4427.	6.7	102
48	Guanidinium-Based Ionic Covalent Organic Framework for Rapid and Selective Removal of Toxic Cr(VI) Oxoanions from Water. Environmental Science & Technology, 2019, 53, 878-883.	10.0	101
49	Au on MgAl2O4 spinels: The effect of support surface properties in glycerol oxidation. Journal of Catalysis, 2010, 275, 108-116.	6.2	100
50	Resolving the Amorphous Structure of Lithium Phosphorus Oxynitride (Lipon). Journal of the American Chemical Society, 2018, 140, 11029-11038.	13.7	99
51	Unraveling the Nanoscale Heterogeneity of Solid Electrolyte Interphase Using Tip-Enhanced Raman Spectroscopy. Joule, 2019, 3, 2001-2019.	24.0	99
52	Nanoparticles of gold on -AlO produced by dc magnetron sputtering. Journal of Catalysis, 2005, 231, 151-158.	6.2	95
53	The electrochemical reactions of pure indium with Li and Na: Anomalous electrolyte decomposition, benefits of FEC additive, phase transitions and electrode performance. Journal of Power Sources, 2014, 248, 1105-1117.	7.8	93
54	Efficient CO ₂ Capture by Porous, Nitrogenâ€Doped Carbonaceous Adsorbents Derived from Taskâ€5pecific Ionic Liquids. ChemSusChem, 2012, 5, 1912-1917.	6.8	92

#	Article	IF	CITATIONS
55	High voltage stability of LiCoO2 particles with a nano-scale Lipon coating. Electrochimica Acta, 2011, 56, 6573-6580.	5.2	91
56	Nanoscale Imaging of Whole Cells Using a Liquid Enclosure and a Scanning Transmission Electron Microscope. PLoS ONE, 2009, 4, e8214.	2.5	90
57	AlSb thin films as negative electrodes for Li-ion and Na-ion batteries. Journal of Power Sources, 2013, 243, 699-705.	7.8	89
58	A "Shipâ€Inâ€Aâ€Bottle―Approach to Synthesis of Polymer Dots@Silica or Polymer Dots@Carbon Coreâ€Sh Nanospheres. Advanced Materials, 2012, 24, 6017-6021.	e 21.0	88
59	Soluble Porous Coordination Polymers by Mechanochemistry: From Metalâ€Containing Films/Membranes to Active Catalysts for Aerobic Oxidation. Advanced Materials, 2015, 27, 234-239.	21.0	88
60	Understanding the Role of NH ₄ F and Al ₂ O ₃ Surface Co-modification on Lithium-Excess Layered Oxide Li _{1.2} Ni _{0.2} Mn _{0.6} O ₂ . ACS Applied Materials & amp; Interfaces, 2015, 7, 19189-19200.	8.0	87
61	Robust Solid/Electrolyte Interphase (SEI) Formation on Si Anodes Using Glyme-Based Electrolytes. ACS Energy Letters, 2021, 6, 1684-1693.	17.4	87
62	Constructing Hierarchical Interfaces: TiO ₂ -Supported PtFe–FeO _{<i>x</i>} Nanowires for Room Temperature CO Oxidation. Journal of the American Chemical Society, 2015, 137, 10156-10159.	13.7	86
63	Preparation and CO2 adsorption properties of soft-templated mesoporous carbons derived from chestnut tannin precursors. Microporous and Mesoporous Materials, 2016, 222, 94-103.	4.4	86
64	Low-Thermal-Budget Photonic Processing of Highly Conductive Cu Interconnects Based on CuO Nanoinks: Potential for Flexible Printed Electronics. ACS Applied Materials & Interfaces, 2016, 8, 2441-2448.	8.0	83
65	Quantitative Electrochemical Measurements Using <i>In Situ</i> ec-S/TEM Devices. Microscopy and Microanalysis, 2014, 20, 452-461.	0.4	80
66	Evaluating the solid electrolyte interphase formed on silicon electrodes: a comparison of ex situ X-ray photoelectron spectroscopy and in situ neutron reflectometry. Physical Chemistry Chemical Physics, 2016, 18, 13927-13940.	2.8	80
67	Anomalous Discharge Product Distribution in Lithium-Air Cathodes. Journal of Physical Chemistry C, 2012, 116, 8401-8408.	3.1	79
68	Atmospheric Pressure Scanning Transmission Electron Microscopy. Nano Letters, 2010, 10, 1028-1031.	9.1	77
69	Effect of Morphology and Manganese Valence on the Voltage Fade and Capacity Retention of Li[Li _{2/12} Ni _{3/12} Mn _{7/12}]O ₂ . ACS Applied Materials & Interfaces, 2014, 6, 18868-18877.	8.0	76
70	An Artificial Solid Electrolyte Interphase Enables the Use of a LiNi _{0.5} Mn _{1.5} O ₄ 5 V Cathode with Conventional Electrolytes. Advanced Energy Materials, 2013, 3, 1275-1278.	19.5	75
71	Gold on carbon: one billion catalysts under a single label. Physical Chemistry Chemical Physics, 2012, 14, 2969.	2.8	74
72	Lithium malonatoborate additives enabled stable cycling of 5 V lithium metal and lithium ion batteries. Nano Energy, 2017, 40, 9-19.	16.0	72

#	Article	IF	CITATIONS
73	Fabrication and characterization of Li–Mn–Ni–O sputtered thin film high voltage cathodes for Li-ion batteries. Journal of Power Sources, 2012, 211, 108-118.	7.8	71
74	New Tricks for Old Molecules: Development and Application of Porous Nâ€doped, Carbonaceous Membranes for CO ₂ Separation. Advanced Materials, 2013, 25, 4152-4158.	21.0	71
75	Magnetron sputtering of gold nanoparticles onto WO3 and activated carbon. Catalysis Today, 2007, 122, 248-253.	4.4	68
76	In Situ Determination of the Liquid/Solid Interface Thickness and Composition for the Li Ion Cathode LiMn _{1.5} Ni _{0.5} O ₄ . ACS Applied Materials & Interfaces, 2014, 6, 18569-18576.	8.0	68
77	Role of pH in the Formation of Structurally Stable and Catalytically Active TiO ₂ -Supported Gold Catalysts. Journal of Physical Chemistry C, 2009, 113, 269-280.	3.1	67
78	The reaction mechanism of FeSb2 as anode for sodium-ion batteries. Physical Chemistry Chemical Physics, 2014, 16, 9538.	2.8	65
79	Dynamic Lithium Distribution upon Dendrite Growth and Shorting Revealed by Operando Neutron Imaging. ACS Energy Letters, 2019, 4, 2402-2408.	17.4	65
80	Real space imaging of the microscopic origins of the ultrahigh dielectric constant in polycrystalline CaCu3Ti4O12. Applied Physics Letters, 2005, 86, 102902.	3.3	64
81	Probing the Mechanism of Sodium Ion Insertion into Copper Antimony Cu ₂ Sb Anodes. Journal of Physical Chemistry C, 2014, 118, 7856-7864.	3.1	64
82	Ambient Lithium–SO ₂ Batteries with Ionic Liquids as Electrolytes. Angewandte Chemie - International Edition, 2014, 53, 2099-2103.	13.8	62
83	AuPd-nNiO as an effective catalyst for the base-free oxidation of HMF under mild reaction conditions. Green Chemistry, 2019, 21, 4090-4099.	9.0	62
84	Influence of Hydrocarbon and CO ₂ on the Reversibility of Li–O ₂ Chemistry Using <i>In Situ</i> Ambient Pressure X-ray Photoelectron Spectroscopy. Journal of Physical Chemistry C, 2013, 117, 25948-25954.	3.1	59
85	Unraveling manganese dissolution/deposition mechanisms on the negative electrode in lithium ion batteries. Physical Chemistry Chemical Physics, 2014, 16, 10398.	2.8	59
86	Acidâ€Functionalized Mesoporous Carbon: An Efficient Support for Ruthenium atalyzed γâ€Valerolactone Production. ChemSusChem, 2015, 8, 2520-2528.	6.8	58
87	A POM–organic framework anode for Li-ion battery. Journal of Materials Chemistry A, 2015, 3, 22989-22995.	10.3	58
88	Aromatic Polyimide/Graphene Composite Organic Cathodes for Fast and Sustainable Lithiumâ€lon Batteries. ChemSusChem, 2018, 11, 763-772.	6.8	58
89	Au on Nanosized NiO: A Cooperative Effect between Au and Nanosized NiO in the Baseâ€Free Alcohol Oxidation. ChemCatChem, 2011, 3, 1612-1618.	3.7	57
90	Influence of Periodic Nitrogen Functionality on the Selective Oxidation of Alcohols. Chemistry - an Asian Journal, 2012, 7, 387-393.	3.3	57

#	Article	IF	CITATIONS
91	Vacuum-Assisted Low-Temperature Synthesis of Reduced Graphene Oxide Thin-Film Electrodes for High-Performance Transparent and Flexible All-Solid-State Supercapacitors. ACS Applied Materials & Interfaces, 2018, 10, 11008-11017.	8.0	57
92	Current Collectors for Rechargeable Li-Air Batteries. Journal of the Electrochemical Society, 2011, 158, A658-A663.	2.9	56
93	Direct measurement of the chemical reactivity of silicon electrodes with LiPF6-based battery electrolytes. Chemical Communications, 2014, 50, 3081.	4.1	56
94	The Cell-in-Series Method: A Technique for Accelerated Electrode Degradation in Redox Flow Batteries. Journal of the Electrochemical Society, 2016, 163, A5202-A5210.	2.9	54
95	Using supported Au nanoparticles as starting material for preparing uniform Au/Pd bimetallic catalysts. Physical Chemistry Chemical Physics, 2010, 12, 2183.	2.8	51
96	Nitrogenâ€Enriched Carbons from Alkali Salts with High Coulombic Efficiency for Energy Storage Applications. Advanced Energy Materials, 2013, 3, 708-712.	19.5	51
97	A Perspective on Coatings to Stabilize High-Voltage Cathodes: LiMn _{1.5} Ni _{0.5} O ₄ with Sub-Nanometer Lipon Cycled with LiPF ₆ Electrolyte. Journal of the Electrochemical Society, 2013, 160, A3113-A3125.	2.9	51
98	Ionic liquid derived carbons as highly efficient oxygen reduction catalysts: first elucidation of pore size distribution dependent kinetics. Chemical Communications, 2014, 50, 1469-1471.	4.1	49
99	Intrinsic chemical reactivity of solid-electrolyte interphase components in silicon–lithium alloy anode batteries probed by FTIR spectroscopy. Journal of Materials Chemistry A, 2020, 8, 7897-7906.	10.3	49
100	An efficient low-temperature route to nitrogen-doping and activation of mesoporous carbons for CO ₂ capture. Chemical Communications, 2015, 51, 17261-17264.	4.1	47
101	Synthesis of Porous, Nitrogenâ€Doped Adsorption/Diffusion Carbonaceous Membranes for Efficient CO ₂ Separation. Macromolecular Rapid Communications, 2013, 34, 452-459.	3.9	46
102	Degradation mechanisms of lithium-rich nickel manganese cobalt oxide cathode thin films. RSC Advances, 2014, 4, 23364.	3.6	45
103	Bismuth as a modifier of Au–Pd catalyst: Enhancing selectivity in alcohol oxidation by suppressing parallel reaction. Journal of Catalysis, 2012, 292, 73-80.	6.2	44
104	Phosphorylated mesoporous carbon as effective catalyst for the selective fructose dehydration to HMF. Journal of Energy Chemistry, 2013, 22, 305-311.	12.9	44
105	Accelerating Membraneâ€based CO ₂ Separation by Soluble Nanoporous Polymer Networks Produced by Mechanochemical Oxidative Coupling. Angewandte Chemie - International Edition, 2018, 57, 2816-2821.	13.8	44
106	The Study of the Binder Poly(acrylic acid) and Its Role in Concomitant Solid–Electrolyte Interphase Formation on Si Anodes. ACS Applied Materials & Interfaces, 2020, 12, 10018-10030.	8.0	44
107	Synthesis and Characterization of Lithium Bis(fluoromalonato)borate for Lithiumâ€lon Battery Applications. Advanced Energy Materials, 2014, 4, 1301368.	19.5	43
108	Solid-State Synthesis of Conjugated Nanoporous Polycarbazoles. ACS Macro Letters, 2017, 6, 1056-1059.	4.8	42

#	Article	IF	CITATIONS
109	Electrochemical Reactivity and Passivation of Silicon Thin-Film Electrodes in Organic Carbonate Electrolytes. ACS Applied Materials & Interfaces, 2020, 12, 40879-40890.	8.0	42
110	NiO as a peculiar support for metal nanoparticles in polyols oxidation. Catalysis Science and Technology, 2013, 3, 394-399.	4.1	40
111	The Influence of Local Distortions on Proton Mobility in Acceptor Doped Perovskites. Chemistry of Materials, 2018, 30, 4919-4925.	6.7	40
112	Properties of lithium phosphorus oxynitride (Lipon) for 3D solid-state lithium batteries. Journal of Materials Research, 2010, 25, 1507-1515.	2.6	39
113	Predictions of particle size and lattice diffusion pathway requirements for sodium-ion anodes using ÎCu6Sn5 thin films as a model system. Physical Chemistry Chemical Physics, 2013, 15, 10885.	2.8	38
114	Rational Design of Lithium–Sulfur Battery Cathodes Based on Experimentally Determined Maximum Active Material Thickness. Journal of the American Chemical Society, 2017, 139, 9229-9237.	13.7	38
115	Investigations of Sr3Fe2â^xMnxO7â^î´the n=2 Ruddlesden–Popper phases with d3/d4 interactions. Solid State Sciences, 2000, 2, 513-522.	0.7	37
116	Shear Thickening Electrolytes for High Impact Resistant Batteries. ACS Energy Letters, 2017, 2, 2084-2088.	17.4	37
117	2Flux growth and characterization of Ce-substituted <mml:math xmlns:mml="http://www.w3.org/1998/Math/MathML" altimg="si0047.gif" overflow="scroll"><mml:mrow><mml:msub><mml:mrow><mml:mi>Nd</mml:mi></mml:mrow><mml:mrow><mml:mi>Nd</mml:mi></mml:mrow><mml:mrow><mml:math>> single crystals. Journal of Magnetism</mml:math></mml:mrow></mml:msub></mml:mrow></mml:math 	זיייייייייייייייייייייייייייייייייייי	ชดl:mn> </td
118	and Magnetic Materials, 2017, 434, 19. Probing microstructure and electrolyte concentration dependent cell chemistry <i>via operando</i> small angle neutron scattering. Energy and Environmental Science, 2019, 12, 1866-1877.	30.8	36
119	Elucidating Interfacial Stability between Lithium Metal Anode and Li Phosphorus Oxynitride via <i>In Situ</i> Electron Microscopy. Nano Letters, 2021, 21, 151-157.	9.1	36
120	Role of Hydroxyl Groups on the Stability and Catalytic Activity of Au Clusters on a Rutile Surface. Journal of Physical Chemistry Letters, 2011, 2, 2918-2924.	4.6	35
121	Cas evolution from cathode materials: A pathway to solvent decomposition concomitant to SEI formation. Journal of Power Sources, 2013, 239, 341-346.	7.8	34
122	Evidence for the Formation of Nitrogen-Rich Platinum and Palladium Nitride Nanoparticles. Chemistry of Materials, 2013, 25, 4936-4945.	6.7	33
123	Multifunctional approaches for safe structural batteries. Journal of Energy Storage, 2021, 40, 102747.	8.1	33
124	Influence of Support Hydroxides on the Catalytic Activity of Oxidized Gold Clusters. ChemCatChem, 2010, 2, 281-286.	3.7	32
125	Superacid-promoted synthesis of highly porous hypercrosslinked polycarbazoles for efficient CO ₂ capture. Chemical Communications, 2017, 53, 7645-7648.	4.1	32
126	Ambient Temperature Graphitization Based on Mechanochemical Synthesis. Angewandte Chemie - International Edition, 2020, 59, 21935-21939.	13.8	32

#	Article	IF	CITATIONS
127	The local atomic structure and chemical bonding in sodium tin phases. Journal of Materials Chemistry A, 2014, 2, 18959-18973.	10.3	31
128	Bis(fluoromalonato)borate (BFMB) anion based ionic liquid as an additive for lithium-ion battery electrolytes. Journal of Materials Chemistry A, 2014, 2, 7606-7614.	10.3	31
129	Synthesis of Ni-Rich Thin-Film Cathode as Model System for Lithium Ion Batteries. ACS Applied Energy Materials, 2019, 2, 1405-1412.	5.1	31
130	Intrinsic Surface Stability in LiMn2–xNixO4–Î′ (x = 0.45, 0.5) High Voltage Spinel Materials for Lithium Ion Batteries. Electrochemical and Solid-State Letters, 2012, 15, A72.	2.2	30
131	Type I Clathrates as Novel Silicon Anodes: An Electrochemical and Structural Investigation. Advanced Science, 2015, 2, 1500057.	11.2	30
132	PdH _{<i>x</i>} Entrapped in a Covalent Triazine Framework Modulates Selectivity in Glycerol Oxidation. ChemCatChem, 2015, 7, 2149-2154.	3.7	30
133	A new family of fluidic precursors for the self-templated synthesis of hierarchical nanoporous carbons. Chemical Communications, 2013, 49, 7289.	4.1	29
134	Evaluation of the physi- and chemisorption of hydrogen in alkali (Na, Li) doped fullerenes. International Journal of Hydrogen Energy, 2015, 40, 2710-2716.	7.1	29
135	Formation of Iron Oxyfluoride Phase on the Surface of Nano-Fe3O4 Conversion Compound for Electrochemical Energy Storage. Journal of Physical Chemistry Letters, 2013, 4, 3798-3805.	4.6	28
136	Structure of Spontaneously Formed Solid-Electrolyte Interphase on Lithiated Graphite Determined Using Small-Angle Neutron Scattering. Journal of Physical Chemistry C, 2015, 119, 9816-9823.	3.1	28
137	Probing Electrolyte Solvents at Solid/Liquid Interface Using Gap-Mode Surface-Enhanced Raman Spectroscopy. Journal of the Electrochemical Society, 2019, 166, A178-A187.	2.9	28
138	Metastable Li _{1+l̂´} Mn ₂ O ₄ (0 â‰ቑ̂ ≤) Spinel Phases Revealed by in Operando Neutron Diffraction and First-Principles Calculations. Chemistry of Materials, 2019, 31, 124-134.	6.7	28
139	Structural Degradation of High Voltage Lithium Nickel Manganese Cobalt Oxide (NMC) Cathodes in Solid-State Batteries and Implications for Next Generation Energy Storage. ACS Applied Energy Materials, 2020, 3, 1768-1774.	5.1	28
140	Properties of the perovskites, SrMn1â^'xFexO3â^'δ (x=1/3, 1/2, 2/3). Solid State Sciences, 2000, 2, 821-831.	3.2	27
141	The electrochemical reactions of SnO2 with Li and Na: A study using thin films and mesoporous carbons. Journal of Power Sources, 2015, 284, 1-9.	7.8	27
142	Synthesis and characterization of the oxynitride pyrochlore - Sm2Mo2O3.83N3.17. Materials Research Bulletin, 2001, 36, 1521-1530.	5.2	26
143	Oxygen and CO Adsorption on Au/SiO ₂ Catalysts Prepared by Magnetron Sputtering: The Role of Oxygen Storage. Industrial & Engineering Chemistry Research, 2010, 49, 10428-10437.	3.7	26
144	Composition Dependence of the Pore Structure and Water Transport of Composite Catalyst Layers for Polymer Electrolyte Fuel Cells. Journal of the Electrochemical Society, 2013, 160, F1000-F1005.	2.9	26

#	Article	IF	CITATIONS
145	Correlating Local Structure with Electrochemical Activity in Li ₂ MnO ₃ . Journal of Physical Chemistry C, 2015, 119, 18022-18029.	3.1	26
146	Chemistry of Sputter-Deposited Lithium Sulfide Films. Journal of the American Chemical Society, 2017, 139, 10669-10676.	13.7	26
147	Probing battery chemistry with liquid cell electron energy loss spectroscopy. Chemical Communications, 2015, 51, 16377-16380.	4.1	25
148	A sodium–aluminum hybrid battery. Journal of Materials Chemistry A, 2017, 5, 6589-6596.	10.3	25
149	Silicon Surface Tethered Polymer as Artificial Solid Electrolyte Interface. Scientific Reports, 2018, 8, 11549.	3.3	25
150	Toward quantifying capacity losses due to solid electrolyte interphase evolution in silicon thin film batteries. Journal of Chemical Physics, 2020, 152, 084702.	3.0	25
151	Distilling nanoscale heterogeneity of amorphous silicon using tip-enhanced Raman spectroscopy (TERS) via multiresolution manifold learning. Nature Communications, 2021, 12, 578.	12.8	25
152	Electronic, Magnetic, and Magnetoresistance Properties of the n=2 Ruddlesden–Popper Phases Sr3Fe2â°'xCoxO7Ⱂδ (0.25â‰æâ‰≇.75). Journal of Solid State Chemistry, 2002, 166, 292-304.	2.9	24
153	Fluorination of "brick and mortar―soft-templated graphitic ordered mesoporous carbons for high power lithium-ion battery. Journal of Materials Chemistry A, 2013, 1, 9414.	10.3	23
154	Activity and Evolution of Vapor Deposited Pt-Pd Oxygen Reduction Catalysts for Solid Acid Fuel Cells. Journal of the Electrochemical Society, 2013, 160, F175-F182.	2.9	23
155	Bottom up synthesis of boron-doped graphene for stable intermediate temperature fuel cell electrodes. Carbon, 2017, 123, 605-615.	10.3	23
156	Si Oxidation and H ₂ Gassing During Aqueous Slurry Preparation for Li-Ion Battery Anodes. Journal of Physical Chemistry C, 2018, 122, 9746-9754.	3.1	23
157	Synthesis and Electrochemical and Structural Investigations of Oxidatively Stable Li ₂ MoO ₃ and <i>x</i> Li ₂ MoO ₃ ·(1 –) Tj ETQq1 1 0.7843	146rgBT /(Dv ed ock 10 T
158	Intrinsic Chemical Reactivity of Silicon Electrode Materials: Gas Evolution. Chemistry of Materials, 2020, 32, 3199-3210.	6.7	23
159	Synthesis and Characterization of Sr3FeMoO6.88:Â An Oxygen-Deficient 2D Analogue of the Double Perovskite Sr2FeMoO6. Chemistry of Materials, 2005, 17, 2562-2567.	6.7	22
160	"One-pot―synthesis of phosphorylated mesoporous carbon heterogeneous catalysts with tailored surface acidity. Catalysis Today, 2012, 186, 12-19.	4.4	22
161	Identifying the Role of Nâ€Heteroatom Location in the Activity of Metal Catalysts for Alcohol Oxidation. ChemCatChem, 2015, 7, 1338-1346.	3.7	22
162	Defect-Accommodating Intermediates Yield Selective Low-Temperature Synthesis of YMnO ₃ Polymorphs. Inorganic Chemistry, 2020, 59, 13639-13650.	4.0	22

#	Article	IF	CITATIONS
163	Physical vapor deposition process for engineering Pt based oxygen reduction reaction catalysts on NbOx templated carbon support. Journal of Power Sources, 2020, 451, 227709.	7.8	22
164	Synthesis and characterization of the new Ln2FeMoO7 (Ln = Y, Dy, Ho) compounds. Journal of Materials Chemistry, 2004, 14, 1623.	6.7	21
165	Directed Synthesis of Nanoporous Carbons from Taskâ€5pecific Ionic Liquid Precursors for the Adsorption of CO ₂ . ChemSusChem, 2014, 7, 3284-3289.	6.8	21
166	Energetics of Na ⁺ Transport through the Electrode/Cathode Interface in Single Solvent Electrolytes. Journal of the Electrochemical Society, 2017, 164, A580-A586.	2.9	21
167	Direct Measure of Electrode Spatial Heterogeneity: Influence of Processing Conditions on Anode Architecture and Performance. ACS Applied Materials & Interfaces, 2020, 12, 55954-55970.	8.0	21
168	Properties of the n=3 Ruddlesden–Popper Phases Sr4Mn3â^'xFexO10â^'δ (x=1, 1.5, 2). Journal of Solid State Chemistry, 2000, 155, 96-104.	2.9	20
169	The confinement effect on the activity of Au NPs in polyol oxidation. Catalysis Science and Technology, 2016, 6, 598-601.	4.1	20
170	Depressing the hydrogenation and decomposition reaction in H ₂ O ₂ synthesis by supporting AuPd on oxygen functionalized carbon nanofibers. Catalysis Science and Technology, 2016, 6, 694-697.	4.1	20
171	Catalytic Activity of Tiâ€based MXenes for the Hydrogenation of Furfural. ChemCatChem, 2020, 12, 5733-5742.	3.7	20
172	Toward Quantitative Electrochemical Measurements on the Nanoscale by Scanning Probe Microscopy: Environmental and Current Spreading Effects. ACS Nano, 2013, 7, 8175-8182.	14.6	19
173	Shear Thickening Electrolyte Built from Sterically Stabilized Colloidal Particles. ACS Applied Materials & Interfaces, 2018, 10, 9424-9434.	8.0	19
174	Understanding Binder–Silicon Interactions during Slurry Processing. Journal of Physical Chemistry C, 2020, 124, 13479-13494.	3.1	19
175	In situ growth synthesis of heterostructured LnPO4–SiO2 (Ln = La, Ce, and Eu) mesoporous materials as supports for small gold particles used in catalytic CO oxidation. Journal of Materials Chemistry, 2012, 22, 25227.	6.7	18
176	Influence of Nonstoichiometry on Proton Conductivity in Thin-Film Yttrium-Doped Barium Zirconate. ACS Applied Materials & Interfaces, 2018, 10, 4816-4823.	8.0	18
177	Influence of Binder Coverage on Interfacial Chemistry of Thin Film LiNi _{0.6} Mn _{0.2} Co _{0.2} O ₂ Cathodes. Journal of the Electrochemical Society, 2020, 167, 040521.	2.9	18
178	An anode-free Li metal cell with replenishable Li designed for long cycle life. Energy Storage Materials, 2021, 36, 251-256.	18.0	18
179	Mixed Polyanion Glass Cathodes: Iron Phosphate Vanadate Glasses. Journal of the Electrochemical Society, 2014, 161, A2210-A2215.	2.9	17
180	Investigation on capacity loss mechanisms of lithium-ion pouch cells under mechanical indentation conditions. Journal of Power Sources, 2020, 465, 228314.	7.8	17

#	Article	IF	CITATIONS
181	A detector for neutron imaging. IEEE Transactions on Nuclear Science, 2004, 51, 1016-1019.	2.0	16
182	Vapor Synthesis and Thermal Modification of Supportless Platinum–Ruthenium Nanotubes and Application as Methanol Electrooxidation Catalysts. ACS Applied Materials & Interfaces, 2015, 7, 10115-10124.	8.0	16
183	Investigating the Chemical Reactivity of Lithium Silicate Model SEI Layers. Journal of Physical Chemistry C, 2020, 124, 8153-8161.	3.1	16
184	Examining CO ₂ as an Additive for Solid Electrolyte Interphase Formation on Silicon Anodes. Journal of the Electrochemical Society, 2021, 168, 030534.	2.9	16
185	Critical Evaluation of Potentiostatic Holds as Accelerated Predictors of Capacity Fade during Calendar Aging. Journal of the Electrochemical Society, 2022, 169, 050531.	2.9	16
186	Dry Synthesis of Lithium Intercalated Graphite Powder and Fiber. Journal of the Electrochemical Society, 2014, 161, A614-A619.	2.9	15
187	Lithium Transport in an Amorphous Li _{<i>x</i>} Si Anode Investigated by Quasi-elastic Neutron Scattering. Journal of Physical Chemistry C, 2017, 121, 11083-11088.	3.1	15
188	Role of conductive binder to direct solid–electrolyte interphase formation over silicon anodes. Physical Chemistry Chemical Physics, 2019, 21, 17356-17365.	2.8	15
189	Thin-Film and Bulk Investigations of LiCoBO ₃ as a Li-Ion Battery Cathode. ACS Applied Materials & Interfaces, 2014, 6, 10840-10848.	8.0	14
190	Role of precursor chemistry in the direct fluorination to form titanium based conversion anodes for lithium ion batteries. RSC Advances, 2015, 5, 88876-88885.	3.6	14
191	Interpreting Electrochemical and Chemical Sodiation Mechanisms and Kinetics in Tin Antimony Battery Anodes Using <i>in Situ</i> Transmission Electron Microscopy and Computational Methods. ACS Applied Energy Materials, 2019, 2, 3578-3586.	5.1	14
192	A Topotactic Synthetic Methodology for Highly Fluorineâ€Doped Mesoporous Metal Oxides. Angewandte Chemie - International Edition, 2012, 51, 2888-2893.	13.8	13
193	Predictive Design of Shear-Thickening Electrolytes for Safety Considerations. Journal of the Electrochemical Society, 2017, 164, A2547-A2551.	2.9	13
194	Highâ€Voltage Performance of Niâ€Rich NCA Cathodes: Linking Operating Voltage with Cathode Degradation. ChemElectroChem, 2019, 6, 5571-5580.	3.4	13
195	Bifunctional Ionic Covalent Organic Networks for Enhanced Simultaneous Removal of Chromium(VI) and Arsenic(V) Oxoanions via Synergetic Ion Exchange and Redox Process. Small, 2021, 17, e2104703.	10.0	13
196	Nanostructured carbon electrocatalyst supports for intermediate-temperature fuel cells: Single-walled versus multi-walled structures. Journal of Power Sources, 2017, 337, 145-151.	7.8	12
197	Ru supported on micro and mesoporous carbons as catalysts for biomass-derived molecules hydrogenation. Catalysis Today, 2020, 357, 143-151.	4.4	12
198	Role of silicon-graphite homogeneity as promoted by low molecular weight dispersants. Journal of Power Sources, 2022, 517, 230671.	7.8	12

#	Article	IF	CITATIONS
199	Li2O-Based Cathode Additives Enabling Prelithiation of Si Anodes. Applied Sciences (Switzerland), 2021, 11, 12027.	2.5	12
200	Deposition–Precipitation and Stabilization of a Silica-Supported Au Catalyst by Surface Modification with Carbon Nitride. Catalysis Letters, 2013, 143, 1339-1345.	2.6	11
201	Polyacrylonitrile-based electrolytes: How processing and residual solvent affect ion transport and stability. Journal of Power Sources, 2022, 527, 231165.	7.8	11
202	The use of Magnetron Sputtering for the Production of Heterogeneous Catalysts. Studies in Surface Science and Catalysis, 2006, , 71-78.	1.5	10
203	Sodium Manganese Oxide Thin Films as Cathodes for Na-Ion Batteries. ECS Transactions, 2014, 58, 47-57.	0.5	10
204	Accelerating Membraneâ€based CO ₂ Separation by Soluble Nanoporous Polymer Networks Produced by Mechanochemical Oxidative Coupling. Angewandte Chemie, 2018, 130, 2866-2871.	2.0	10
205	Impact of Fluorination on Phase Stability, Crystal Chemistry, and Capacity of LiCoMnO ₄ High Voltage Spinels. ACS Applied Energy Materials, 2018, 1, 715-724.	5.1	10
206	Ending the Chase for a Perfect Binder: Role of Surface Chemistry Variation and its Influence on Silicon Anodes. ChemElectroChem, 2020, 7, 3790-3797.	3.4	10
207	Evaluating the roles of electrolyte components on the passivation of silicon anodes. Journal of Power Sources, 2022, 523, 231021.	7.8	10
208	Relative Kinetics of Solid-State Reactions: The Role of Architecture in Controlling Reactivity. Journal of the American Chemical Society, 2022, 144, 11975-11979.	13.7	10
209	Lithium Vanadium Oxide (Li _{1.1} V ₃ O ₈) Coated with Amorphous Lithium Phosphorous Oxynitride (LiPON): Role of Material Morphology and Interfacial Structure on Resulting Electrochemistry. Journal of the Electrochemical Society, 2017, 164, A1503-A1513.	2.9	9
210	Active Reaction Control of Cu Redox State Based on Real-Time Feedback from In Situ Synchrotron Measurements. Journal of the American Chemical Society, 2020, 142, 18758-18762.	13.7	9
211	Nanostructured ligament and fiber Al–doped Li7La3Zr2O12 scaffolds to mediate cathode-electrolyte interface chemistry. Journal of Power Sources, 2021, 513, 230551.	7.8	9
212	Competitive adsorption within electrode slurries and impact on cell fabrication and performance. Journal of Power Sources, 2022, 520, 230914.	7.8	9
213	Preparation of Bi Nanowires from the Reaction between Ammonia and Bi1.7V8O16. Chemistry of Materials, 2004, 16, 3348-3351.	6.7	8
214	In-situ liquid and gas transmission electron microscopy of nano-scale materials. Microscopy and Microanalysis, 2012, 18, 1158-1159.	0.4	8
215	Neutron vibrational spectroscopic studies of novel tire-derived carbon materials. Physical Chemistry Chemical Physics, 2017, 19, 22256-22262.	2.8	8
216	Role of Surface Acidity in the Surface Stabilization of the High-Voltage Cathode LiNi _{0.6} Mn _{0.2} Co _{0.2} O ₂ . ACS Omega, 2020, 5, 14968-14975.	3.5	8

#	Article	IF	CITATIONS
217	Amorphous alumina thin films deposited on titanium: Interfacial chemistry and thermal oxidation barrier properties. Physica Status Solidi (A) Applications and Materials Science, 2016, 213, 470-480.	1.8	7
218	Quantification of the ion transport mechanism in protective polymer coatings on lithium metal anodes. Chemical Science, 2021, 12, 7023-7032.	7.4	7
219	Probing Clustering Dynamics between Silicon and PAA or LiPAA Slurries under Processing Conditions. ACS Applied Polymer Materials, 2021, 3, 2447-2460.	4.4	7
220	Role of Low Molecular Weight Polymers on the Dynamics of Silicon Anodes During Casting. ChemPhysChem, 2021, 22, 1049-1058.	2.1	7
221	La ₂ Zr ₂ O ₇ Nanoparticle-Mediated Synthesis of Porous Al-Doped Li ₇ La ₃ Zr ₂ O ₁₂ Garnet. Inorganic Chemistry, 2021, 60, 10012-10021.	4.0	7
222	STEM Studies of Novel Gold Catalysts. Microscopy and Microanalysis, 2008, 14, 306-307.	0.4	6
223	A study of perfluorocarboxylate ester solvents for lithium ion battery electrolytes. Journal of Power Sources, 2015, 299, 434-442.	7.8	6
224	XPCS Microrheology and Rheology of Sterically Stabilized Nanoparticle Dispersions in Aprotic Solvents. ACS Applied Materials & amp; Interfaces, 2021, 13, 14267-14274.	8.0	6
225	Solid Electrolyte Interphase Architecture Determined through In Situ Neutron Scattering. Journal of the Electrochemical Society, 2021, 168, 060523.	2.9	6
226	Role of Pairwise Reactions on the Synthesis of Li _{0.3} La _{0.57} TiO ₃ and the Resulting Structure–Property Correlations. Inorganic Chemistry, 2021, 60, 14831-14843.	4.0	6
227	Understanding the Solution Dynamics and Binding of a PVDF Binder with Silicon, Graphite, and NMC Materials and the Influence on Cycling Performance. ACS Applied Materials & Interfaces, 2022, 14, 23322-23331.	8.0	6
228	Gold nanocatalysts supported on heterostructured PbSO4-MCF mesoporous materials for CO oxidation. Catalysis Communications, 2014, 46, 234-237.	3.3	5
229	Conduction below 100°C in nominal Li6ZnNb4O14. Journal of Materials Science, 2016, 51, 854-860.	3.7	5
230	Hermetically sealed porous-wall hollow microspheres enabled by monolithic glass coatings: Potential for thermal insulation applications. Vacuum, 2022, 195, 110667.	3.5	5
231	Preparation of thin-film neutron converter foils for imaging detectors. IEEE Transactions on Nuclear Science, 2004, 51, 1034-1038.	2.0	3
232	Understanding Catalyst Stability through Aberration-Corrected STEM. Microscopy and Microanalysis, 2009, 15, 1408-1409.	0.4	3
233	Catalytic CO Oxidation Over Gold Nanoparticles: Support Modification by Monolayer- and Submonolayer-Dispersed Sb2O3. Catalysis Letters, 2014, 144, 912-919.	2.6	3
234	Synthesis of metal chloride films: Influence of growth conditions on crystallinity. Thin Solid Films, 2019, 689, 137520.	1.8	3

#	Article	IF	CITATIONS
235	Structure and dynamics of small polyimide oligomers with silicon as a function of aging. Soft Matter, 2021, 17, 7729-7742.	2.7	3
236	Synthesis of model sodium sulfide films. Journal of Vacuum Science and Technology A: Vacuum, Surfaces and Films, 2021, 39, 053404.	2.1	3
237	Stable SEI Formation on Al-Si-Mn Metallic Glass Li-Ion Anode. Journal of the Electrochemical Society, 2021, 168, 100521.	2.9	3
238	Digestion processes and elemental analysis of oxide and sulfide solid electrolytes. Ionics, 2022, 28, 3223-3231.	2.4	3
239	Thin-Film Paradigm to Probe Interfacial Diffusion during Solid-State Metathesis Reactions. Chemistry of Materials, 2022, 34, 6279-6287.	6.7	3
240	Coupling EELS/EFTEM Imaging with Environmental Fluid Cell Microscopy. Microscopy and Microanalysis, 2012, 18, 1104-1105.	0.4	2
241	Magnetron Sputtering to Prepare Supported Metal Catalysts. , 2008, , 347-353.		2
242	Synthesis, Crystal Structure, and Physical Properties of Sr0.93(SixNb1â^'x)Nb10O19 (x=0.87). Journal of Solid State Chemistry, 2000, 152, 540-545.	2.9	1
243	Tuning Electrodeposition Parameters for Tailored Nanoparticle Size, Shape, and Morphology: An In Situ ec-STEM Investigation. Microscopy and Microanalysis, 2014, 20, 1506-1507.	0.4	1
244	Bifunctional Ionic Covalent Organic Networks for Enhanced Simultaneous Removal of Chromium(VI) and Arsenic(V) Oxoanions via Synergetic Ion Exchange and Redox Process (Small 46/2021). Small, 2021, 17, 2170241.	10.0	1
245	A high temperature cell for investigating interfacial structure on the molecular scale in molten salt/alloy systems. Review of Scientific Instruments, 2021, 92, 123903.	1.3	1
246	Synthesis and Characterization of Sr3FeMoO6.88: An Oxygen-Deficient 2D Analogue of the Double Perovskite Sr2FeMoO6 ChemInform, 2005, 36, no.	0.0	0
247	Low-Cost, Atmospheric-Pressure Scanning Transmission Electron Microscopy. Microscopy Today, 2011, 19, 16-20.	0.3	0
248	Carbon Membranes: New Tricks for Old Molecules: Development and Application of Porous Nâ€doped, Carbonaceous Membranes for CO ₂ Separation (Adv. Mater. 30/2013). Advanced Materials, 2013, 25, 4200-4200.	21.0	0
249	In situ Nanoscale Imaging and Spectroscopy of Energy Storage Materials. Microscopy and Microanalysis, 2017, 23, 1964-1965.	0.4	0
250	Multi-modal characterization approach to understand proton transport mechanisms in solid oxide fuel cells. Microscopy and Microanalysis, 2019, 25, 2048-2049.	0.4	0
251	Multi-scale Characterization Study Enabling Deactivation Mechanism in Formed Zeolite Catalyst. Microscopy and Microanalysis, 2020, 26, 1270-1271.	0.4	0
252	Study of Chromium Migration in a Nickel-Based Alloy Using Polarized Neutron Reflectometry and Rutherford Backscattering Spectrometry. Journal of Physical Chemistry C, 2022, 126, 605-610.	3.1	0